N90-12549

EXPERIMENTAL AND NUMERICAL ANALYSES OF LAMINAR BOUNDARY-LAYER FLOW STABILITY OVER AN AIRCRAFT FUSELAGE FOREBODY

Paul M. H. W. Vijgen
University of Kansas
Lawrence, Kansas

Bruce J. Holmes
Head, Flight Applications Branch
NASA Langley Research Center
Hampton, Virginia

PRECEDING PAGE BLANK NOT FILMED

INTRODUCTION

Fuelled by a need to reduce viscous drag of airframes, significant advances have been made in the last decade to design lifting surface geometries with considerable amounts of laminar flow. Advances in production techniques and materials have allowed lifting surface geometries to be within required tolerances for laminar flow. Both availability of linear and nonlinear computational boundary-layer stability analysis methods and several recent swept-wing flight tests utilizing advanced transition instrumentation have resulted in definition of a geometric and aerodynamic matrix for applicability of natural laminar flow over swept and unswept wings.

In contrast to the present understanding of practical limits for natural laminar flow over lifting surfaces, limited experimental results are available examining applicability of natural laminar flow over axisymmetric and nonaxisymmetric fuselage shapes at relevantly high length Reynolds numbers. This briefing will show the drag benefits attainable by realizing laminar flow over nonlifting aircraft components such as fuselages and nacelles. A status report is presented on a flight experiment being conducted in cooperation with Cessna Aircraft Company in Wichita, Kansas, to investigate transition location and transition mode over the forward fuselage of a light twin-engine propeller-driven airplane.

Possible application areas for natural laminar flow over nonlifting aircraft components are given in Figure 1.

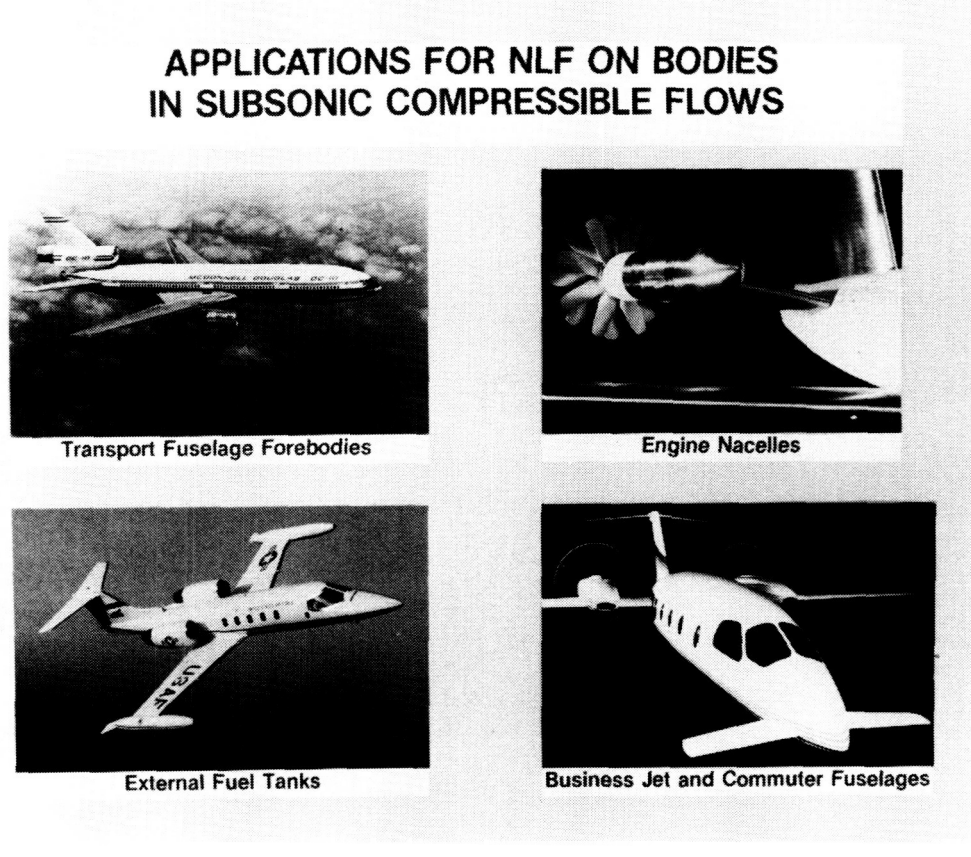

Figure 1

ORIGINAL PAGE
BLACK AND WHITE PHOTOGRAPH

ORIGINAL PAGE IS
OF POOR QUALITY

INTRODUCTION (CONTINUED)

Application of laminar flow to lifting surfaces of transports will increase the relative contribution of the turbulent fuselage to aircraft viscous and total drag (see Figure 2), thus presenting a stimulus to reduce viscous drag of the fuselage. In reference 1 an estimate is presented of the decrease in total aircraft drag when a laminar boundary layer is realized over the above indicated fuselage area. The geometry of the forward fuselage of a typical transport aircraft provides a favorable accelerating pressure gradient from the nose up to the beginning of the cylindrical cabin section on the sides and bottom of the fuselage and after the windshield on top of the fuselage (see reference 2). Additional benefits of a laminar run over the initial portion of the fuselage are a reduction in turbulent drag over the remainder of the fuselage (and possible greater ease of scaling large-eddy break-up devices for turbulent drag reduction) and relief of the wing-fuselage interaction problem. Axisymmetric nacelles of recently introduced high-bypass unducted-fan engines and external fuel tanks can be shaped to sustain large amounts of laminar flow, particularly at compressible flight speeds. Significant runs of laminar flow are predicted in reference 3 for business-jet and commuter-type fuselages when appropriate body shaping is available. At compressible flight conditions (M = 0.60 and up) as much as 30- to 40-percent of the fuselage length is predicted to be capable of sustaining a sufficiently stable laminar boundary layer (reference 1).

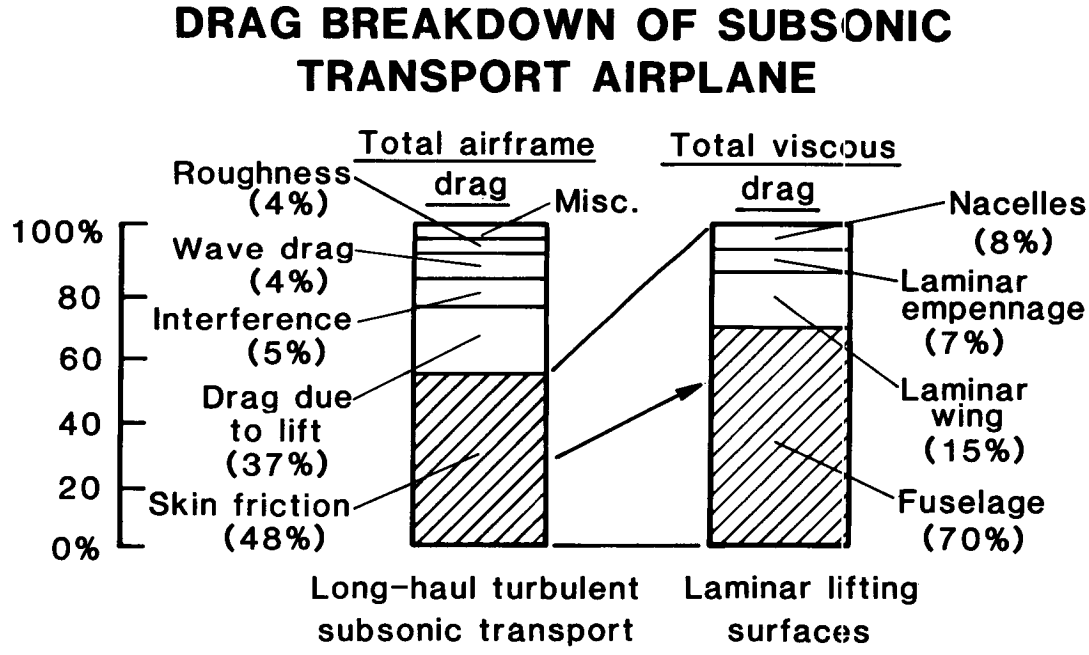

Figure 2

BENEFITS OF NATURAL LAMINAR FLOW

Drag benefit for maintaining laminar flow over the first 30 percent of an advanced business-jet type fuselage can amount to 7-percent in total (viscous and induced) aircraft drag (Figure 3). By comparison, realization of laminar flow over 40 to 50 percent of wing chord results in 12-percent total drag reduction. These drag reductions are compared to fully turbulent configurations. Reference 4 presents a detailed assessment of performance and operating cost improvements for achieving laminar flow over different components of a typical commuter aircraft. Figure 3 also indicates a 2-percent drag reduction for maintaining a laminar boundary layer over turbofan engine nacelles. Reference 5 presents a status report of a flight experiment investigating stability of the laminar boundary layer over a turbofan nacelle under varying acoustical environments.

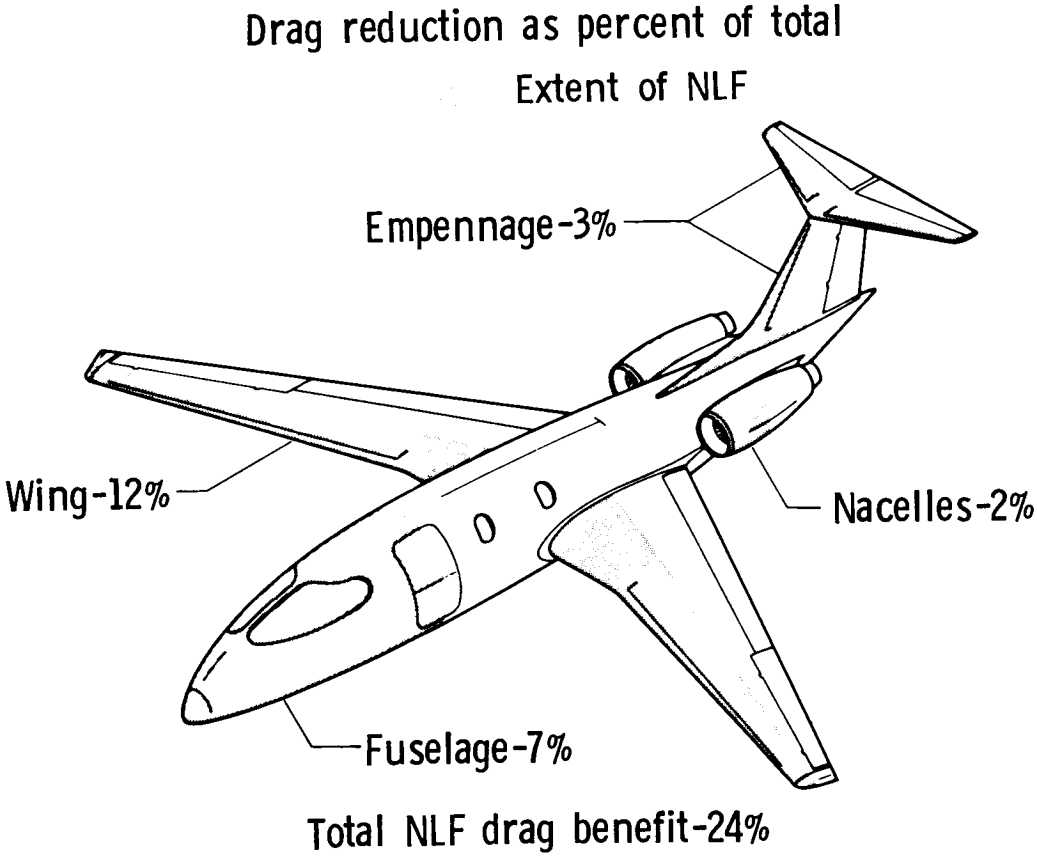

Figure 3

NLF BODY DESIGN CONSIDERATIONS

Figure 4 presents a road map of transition mechanisms that can affect the stability and extent of natural laminar flow over a fuselage. The stability of a laminar boundary layer (in absence of suction or wall cooling) is derived from the magnitude of pressure gradients along the body surface in axial and circumferential directions at a given unit Reynolds number and free-stream Mach number. Energy from sound and turbulence in the environment can be entrained into the laminar boundary layer and lead to increased amplification growth of disturbances in the laminar layer (receptivity problem). Manufacturing excrescences on the fuselage surface can induce strong destabilizing disturbances in the boundary layer, resulting in immediate transition (bypass mechanism), and can generate large local pressure gradients which allow sound and turbulence to be entrained (receptivity).

- Body shape for axial and circumferential pressure gradients (Tollmien-Schlichting and crossflow instabilities)
- Noise and turbulence environment (receptivity)
- Manufacturing tolerances (bypasses)

    - Reynolds number
    - Mach number (flow compressibility)

Figure 4

PAST INCOMPRESSIBLE BODY TRANSITION EXPERIMENTS

Past experimental transition results are mainly available for axisymmetric incompressible (underwater) body shapes. Wind-tunnel results at high subsonic Mach number (Reference 6) pertain to low length Reynolds numbers. Figure 5 presents the measured extent of natural laminar flow (expressed as a transition Reynolds number based on axial length) as a function of the body fineness ratio F_R, defined as ratio of body length to body diameter for incompressible conditions. A decrease of body fineness ratio leads to an increase in axial pressure gradients for a body with constant internal volume. Figure 5 shows that a large increase in the amount of laminar flow is obtained when fineness ratio is reduced. Reference 7 presents results of some of the low-fineness-ratio findings indicated in this figure. Fuselages of business-jet and commuter type aircraft are characterized by fineness ratios of 5 to 9. Figure 5 also shows that limited experimental results are available for axisymmetric shapes in this design area. However, some of the forebody shapes tested are typical for underwater applications. No experimental results are available for nonaxisymmetric geometries at relevant length Reynolds numbers to define practical limits for NLF design factors given in Figure 4.

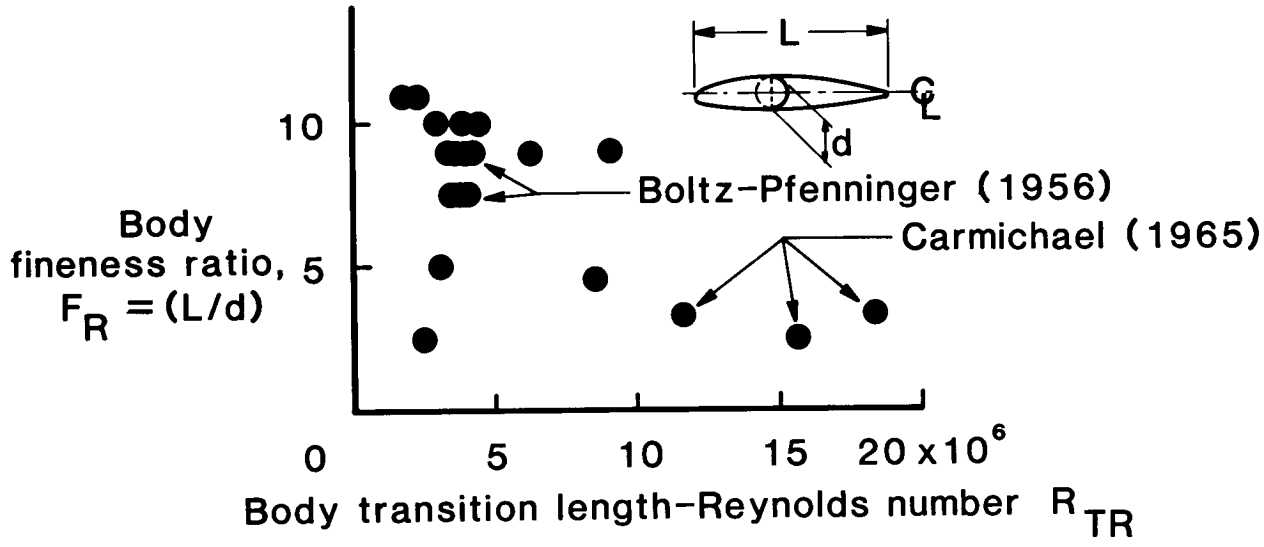

Figure 5

ORIGINAL PAGE IS
OF POOR QUALITY

NASA/CESSNA T-303 NLF FUSELAGE FLIGHT EXPERIMENTS

To investigate the extent and stability of laminar flow over a practical nonaxisymmetric fuselage a flight-test program has been started in cooperation with Cessna Aircraft Company using a Cessna T303 "Crusader" light twin-engine propeller-driven aircraft (Figure 6). Preliminary analysis of axial pressure gradients over the original fuselage forebody indicated a strong potential for laminar flow in cruise and climb conditions. The indicated nose surface constitutes about 5 percent of the total fuselage wetted area. The production-quality forebody (painted black in Figure 6 for flow-visualization observations) required smoothing with body filler and subsequent sanding of rivet lines and lap joints to prevent premature transition. Proximity of the propeller propulsion system to the forebody allows study of possible effects of propeller and engine noise on mode and location of transition over the fuselage nose. Figure 6 also shows the wing-mounted boom for static and total reference pressures and angle-of-attack and angle-of-sideslip indicators.

Figure 6

ORIGINAL PAGE
BLACK AND WHITE PHOTOGRAPH

T-303 NLF FUSELAGE FLIGHT EXPERIMENT

Installed transition instrumentation on the T303 forebody is given in Figure 7. Pressure port lines along 7 meridian lines measure the pressure field over the nose and possible streamtube effects in the proximity of the propeller plane. Location of transition and extent of the transition process is measured by 3 lines of staggered surface hot films, one line on top, port and starboard side of the fuselage nose respectively. The signal-to-noise characteristics of these high-impedance hot films will allow spectral analysis of the signal to identify energy distribution in the frequency domain of each hot film. To identify and quantify the external environment to which the laminar boundary layer is subjected, 3 flush mounted microphones are installed in the nose area and a single-wire free-stream-turbulence probe is mounted near the port wing tip. Engine and propeller power and RPM settings are also measured by the onboard data system.

- 7 surface pressure port lines (140 ports)
  - Nose pressure distribution
  - Propeller streamtube effect
- 39 staggered M&M 50Ω hot films
  - Boundary-layer intermittency
  - Spectral content (T.S. Frequencies)
- 3 Flush mounted B&K microphones
  - Acoustic environment
- TSI freestream turbulence probe
  - Turbulence environment
- Propellers and gas generator RPM and power settings

Figure 7

BOUNDARY-LAYER STABILITY ANALYSIS OVER NONAXISYMMETRIC FUSELAGE FOREBODY

Computational assessment of stability of the laminar boundary layer over the fuselage forebody is carried out along the steps indicated in Figure 8. Inviscid surface pressure distributions are determined for the complete fuselage geometry. Using a quasi-axisymmetric approach the laminar boundary-layer development is determined using a finite-difference scheme. Streamwise Tollmien-Schlichting (T.S.) stability is determined using the boundary-layer profiles calculated by the finite-difference method. In the present briefing only an assessment of the T.S. stability is presented. A full three-dimensional analysis of stability of the laminar boundary layer (i.e., including the effect of boundary-layer cross flow) will be commenced as soon as the required computational tools are available to the authors.

- Inviscid pressure distribution
- Axisymmetric-analogue approach
  - Quasi-axisymmetric boundary-layer analysis
  - Tollmien-Schlichting stability analysis
- Full three-dimensional approach
  - 3-D boundary-layer analysis
  - Tollmien-Schlichting and crossflow stability analysis

Figure 8

T303 FUSELAGE FOREBODY ANALYSIS

Figure 9 shows the inviscid pressure distribution over the T303 forebody as predicted by the VSAERO panel method (Reference 8) at the indicated flight conditions. The pressure contour plots show a moderately favorable pressure gradient (flow acceleration) in the axial direction from the nose (stagnation area) towards the windshield. On top of the fuselage a pressure recovery near the windshield can be observed resulting in an adverse axial pressure gradient towards the windshield. A moderate pressure gradient is predicted in the circumferential direction from the symmetry line to the side of the fuselage. These circumferential gradients will induce curvature of the streamlines and can result in boundary-layer cross flow and possible cross-flow instability.

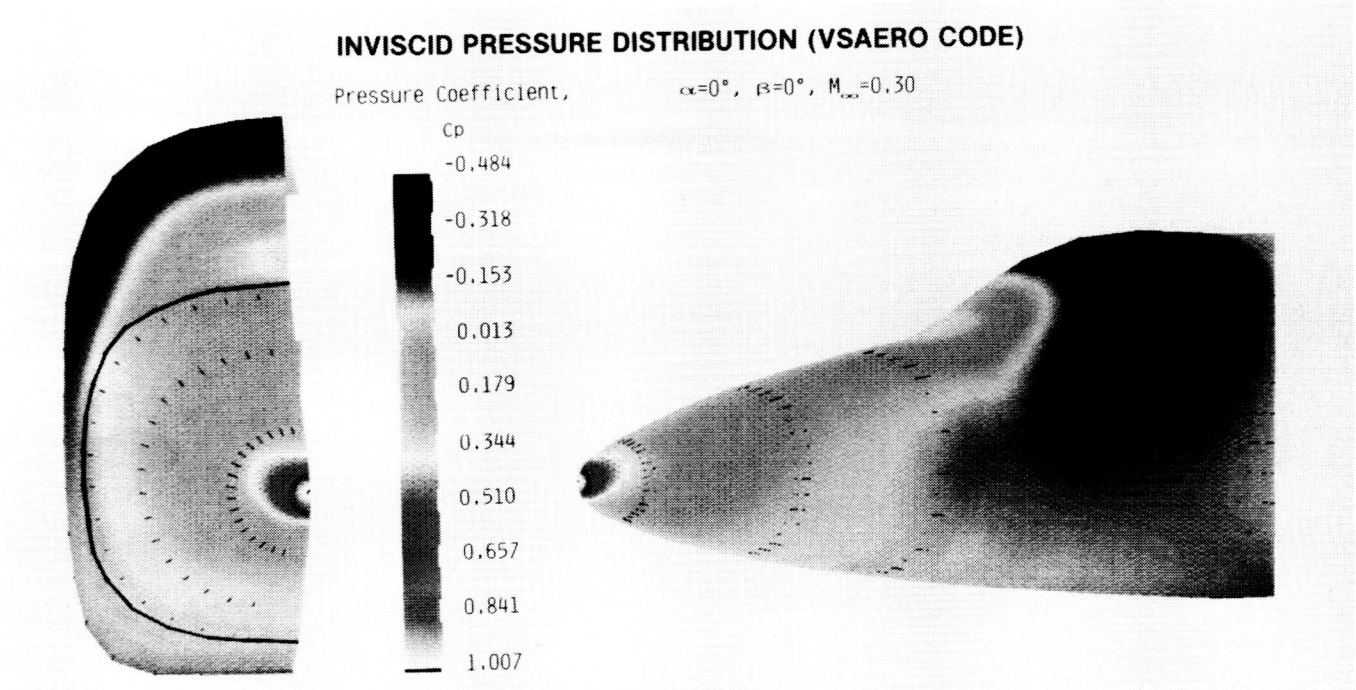

Figure 9

ORIGINAL PAGE
BLACK AND WHITE PHOTOGRAPH

ORIGINAL PAGE IS
OF POOR QUALITY

T303 NLF FUSELAGE FLIGHT EXPERIMENT
COMPARISON OF MEASURED AND CALCULATED PRESSURE DISTRIBUTIONS

Figure 10a presents a comparison of the VSAERO prediction and the measured pressure distribution along meridians at 0 and 45 degrees radials at zero angles of attack and sideslip. Figure 10b gives the comparison for the pressure lines on both sides of the fuselage. A good agreement can be observed between the measurements and the calculations for this flight condition. The effect of a surface wave near the radome joint at FS 44.0 along the 0 degrees radial can be observed in the measured pressure distribution (Figure 10a). The effect of the propellers and propeller-rotation direction on the pressure distribution can be seen in Figure 10b. The rotation sense of both propellers is counter clockwise when looking from the nose to the tail of the fuselage. Consequently, a local acceleration and deceleration is measured near the propeller plane on the port side and starboard side respectively, due to superposition of the propeller-induced flowfield over the basic flowfield over the nose.

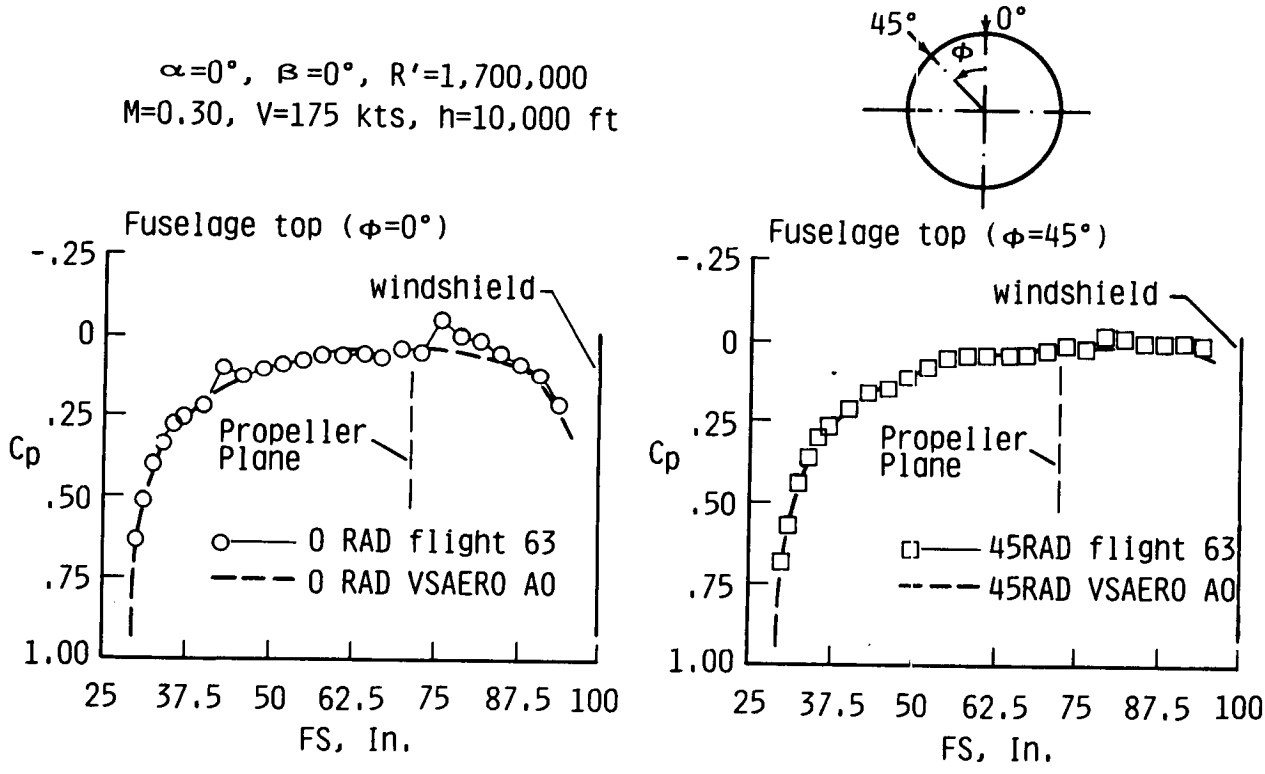

Figure 10a

T303 NLF FUSELAGE FLIGHT EXPERIMENT

Comparison Measured and Calculated Pressure Distributions

α=0°, β=0°, R'=1,700,000
M=0.30, V=175 kts, h=10,000 ft

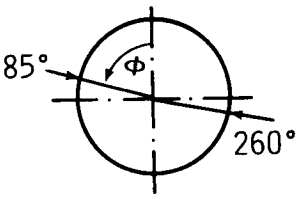

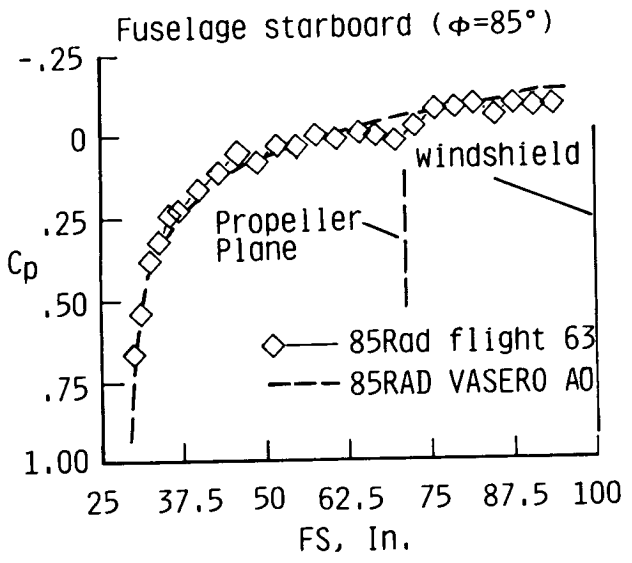

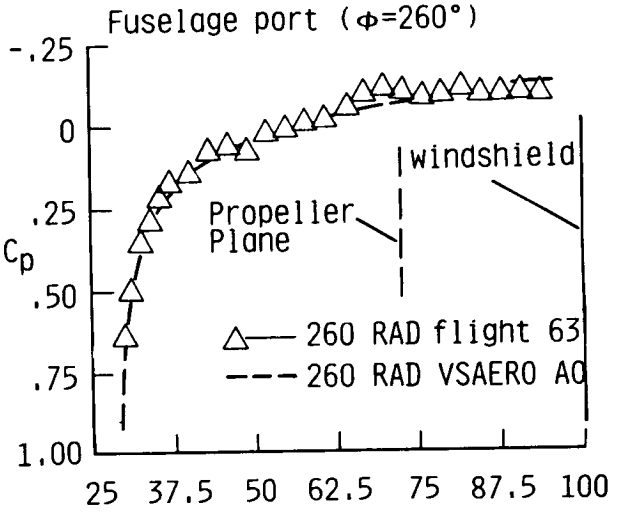

Figure 10b

ORIGINAL PAGE IS
OF POOR QUALITY

T303 FUSELAGE FOREBODY ANALYSIS
INVISCID CROSS-FLOW VELOCITY DISTRIBUTION (VSAERO CODE)

Figure 11 shows the VSAERO prediction of inviscid surface velocities in circumferential directions for two angles of attack (zero sideslip) over the nonaxisymmetric T303 fuselage. At zero angle of attack a line of zero cross flow can be observed near the 45 degree radial position. In the area on top of the fuselage nose between this line and the vertical symmetry plane a circumferential (negative) cross flow towards the symmetry plane is predicted. For radial positions to the left of this line the inviscid circumferential flow is positive. Existence of reversal of inviscid cross-flow vectors presents formidable numerical problems for three-dimensional boundary-layer solvers, as discussed in Reference 9. An increase in angle of attack (see right side of Figure 11) results in an increase in magnitude of circumferential velocities and a shift of the reversal location to the lower quadrant of the fuselage nose. The magnitude of inviscid cross flow and its potential effects on three-dimensional boundary-layer stability can be assessed to first order by relating the magnitude of inviscid cross flow predicted for the fuselage to the cross-flow magnitude over a swept wing. An inviscid cross-flow velocity v_R/U_{inf} = .250 occurs in the leading-edge region of a wing with 15 degrees sweep. From previous laminar-flow experiments on swept wings it is known that cross flow becomes the dominant instability phenomenon only if wing leading-edge sweep is larger than 20 to 25 degrees.

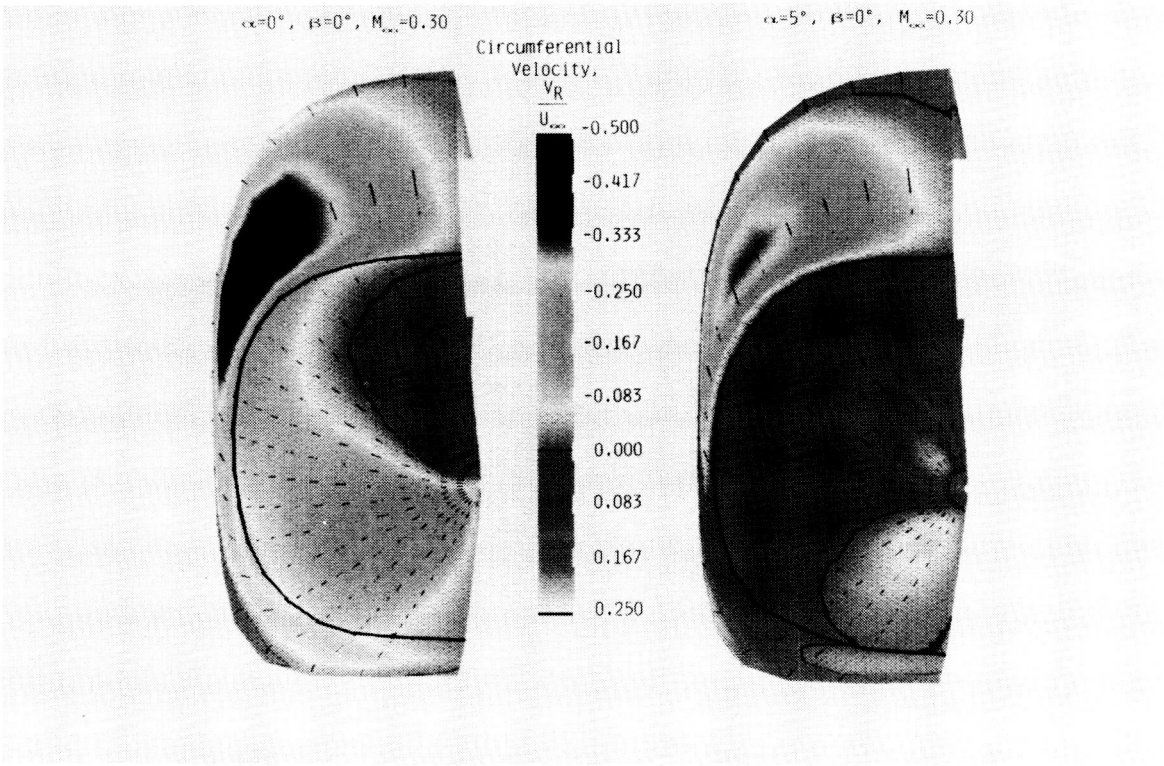

Figure 11

ORIGINAL PAGE
BLACK AND WHITE PHOTOGRAPH

Figure 12a and 12b show the extent of laminar flow and the location of the transition front as indicated by the residue of sublimating chemical (naphthalene) at V = 170 kts at 10,000 ft. On top of the fuselage nose transition occurs about 12 inches ahead of the propeller plane (Figure 12b). Identification of transition extent on the port side of the fuselage was impossible due to roughness transition near the nose during this flight (see figure 12a). Transition extent on the starboard fuselage side (not shown here) is similar to the location on top. Note the effect of sweep of the leading edge of the masking-tape strips, used as coordinate system references, on transition: transition as evidenced by a turbulent wedge occurs 1 to 2 inches behind the beginning of the tape, suggesting a relieving effect on the roughness height as perceived by the laminar boundary layer due to the sweep angle (See Reference 10).

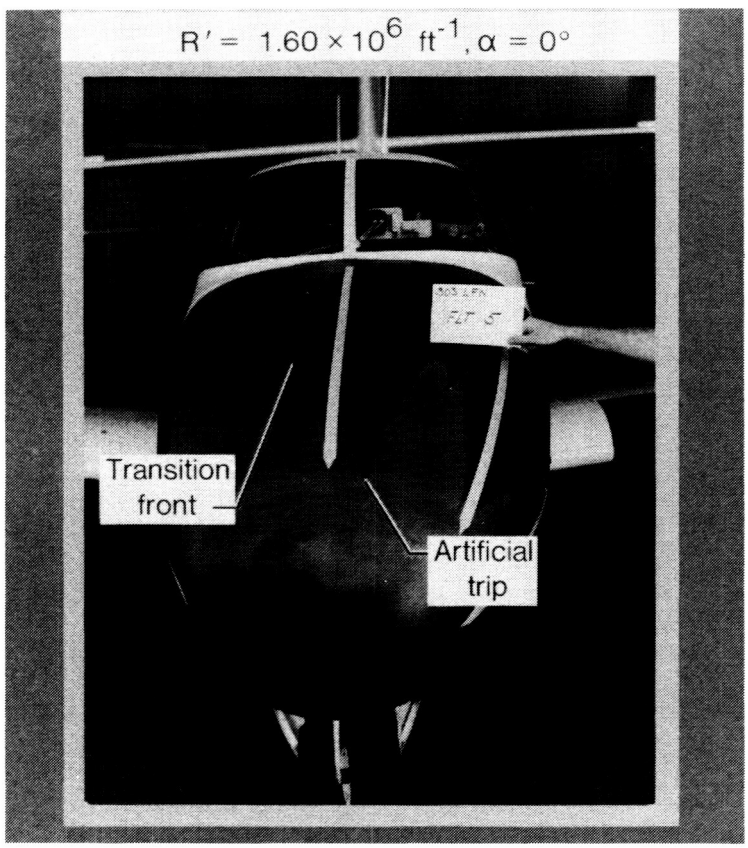

Figure 12a

ORIGINAL PAGE IS
OF POOR QUALITY

ORIGINAL PAGE
BLACK AND WHITE PHOTOGRAPH

Figure 12b

ORIGINAL PAGE IS
OF POOR QUALITY

ORIGINAL PAGE
BLACK AND WHITE PHOTOGRAPH

T303 FUSELAGE FOREBODY ANALYSIS
TOLLMIEN-SCHLICHTING STABILITY ANALYSIS - AXISYMMETRIC ANALOGUE APPROACH

For three streamlines over the top, side, and lower quadrant of the fuselage forebody (indicated as S1, S2 and S3 respectively in Figure 13), boundary-layer development has been calculated using an axisymmetric analogue approach. For each streamline, an equivalent axisymmetric body shape is defined using axial and radial coordinates of the streamline as meridian. This approach is justified in the absence of strong streamline divergence and boundary-layer cross flow (Reference 11). The axisymmetric boundary-layer development along each streamline is calculated using a modified version of Harris's method (Reference 12). Using a spectral method (Reference 13), the incompressible linear Tollmien-Schlichting stability of the laminar boundary layer is determined for each streamline along the body surface for a range of disturbance frequencies at the indicated unit Reynolds number. Figure 13a shows the frequency envelopes for the three streamlines as function of axial nose distance. Most amplified T.S. disturbance frequencies range from 1750 to 3000 Hz for the given flight condition. By comparison, the fundamental propeller and generator turbine frequencies are approximately 100 Hz and 800 Hz, respectively. A logarithmic amplification factor ("n-factor") of 9 is predicted in the region of the propeller plane at R' =1,400,000 at zero angle of attack (Figure 13a). Using the e^n-stability method as a transition prediction tool, and n=9 as criterion for transition onset, transition due to T.S. instability is expected to start near the propeller plane in the absence of exterior disturbances (noise of appropriate frequency and energy levels, free-stream turbulence, and manufacturing imperfections). The observed transition front at a slightly higher unit Reynolds number in Figure 12 corresponds to a calculated "n-factor" of about 6 to 8 in Figure 13a.

Figure 13b shows the calculated T.S. amplification factors along streamlines at an angle of attack of 5 degrees. An "n-factor" of 9 is predicted to occur slightly ahead of the propeller plane over the top of the fuselage forebody, while a lower T.S. instability growth is predicted over the lower quadrant of the nose due to an increased favorable axial pressure gradient at positive angle of attack.

T303 FUSELAGE FOREBODY ANALYSIS

Tollmien-Schlichting Stability Analysis,
Axisymmetric Analogue Approach

M=0.30, R'=1,400,000, α=0°, β=0°
Forebody streamlines (VSAERO)

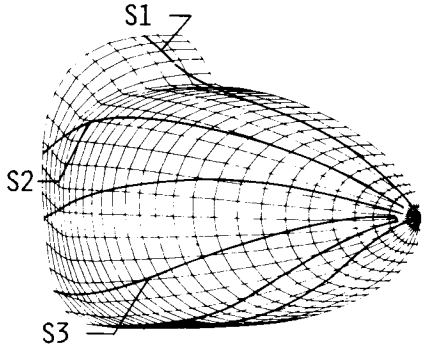

T.S. amplification (Harris-Sallyf)

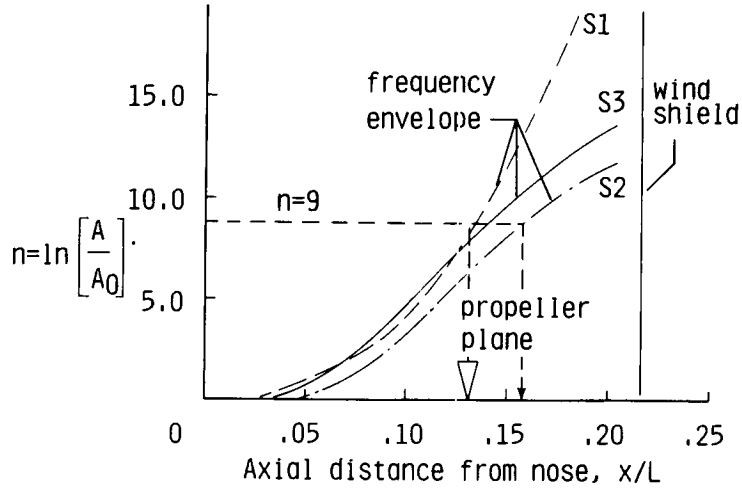

Figure 13a

ORIGINAL PAGE IS
OF POOR QUALITY

Tollmien-Schlichting Stability Analysis,
Axisymmetric Analogue Approach

M=0.30, R'=1,400,000, α=5°, β=0°
Forebody streamlines (VSAERO)

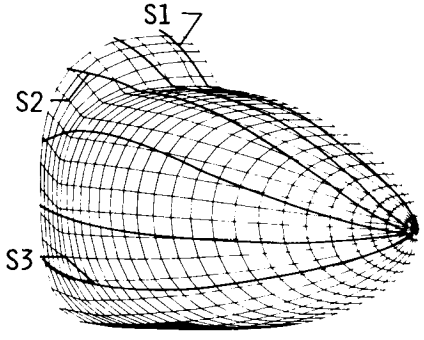

T.S. amplification (Harris-Sallyf)

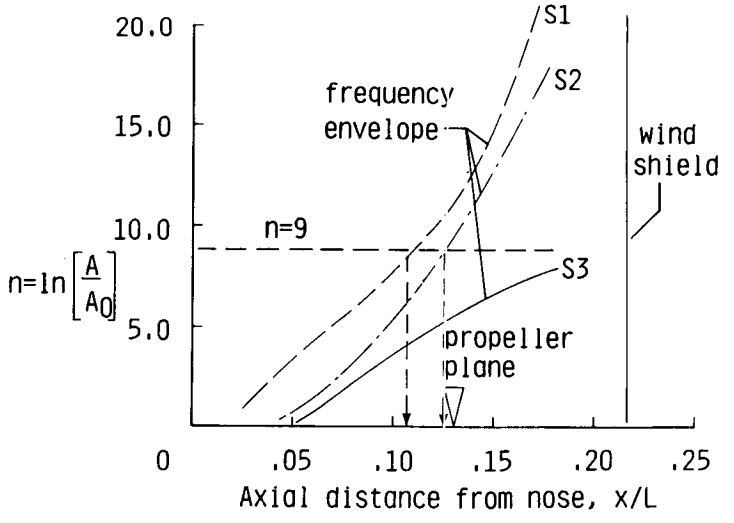

Figure 13b

T303 NLF FUSELAGE FLIGHT EXPERIMENT
HOT-FILM BOUNDARY-LAYER TURBULENCE INTERMITTENCY

Figure 14a and 14b show the observed turbulent intermittency of the hot-film signals over the top and starboard side of the fuselage nose respectively for a flight condition similar to the one shown in Figure 13 (R'=1,700,000). Hot-film intermittency shows transition to occur about 1 foot upstream of the propeller plane (transition location being defined here by 50-percent intermittency) in agreement with the flow visualization pattern. Note a reduction in intermittency from 65 to 50 percent downstream of the propeller plane (indicated by the solid symbol in the intermittency plot) in this flight condition on both top and side of the fuselage nose. The local favorable pressure gradient immediately behind the propeller plane (see Figure 10a and 10b) might explain the observed reduction in turbulence intermittency. Higher turbulent intermittency for the third hot film in both arrays is attributed to turbulent contamination of the previous hot film and its lead wires in the staggered array.

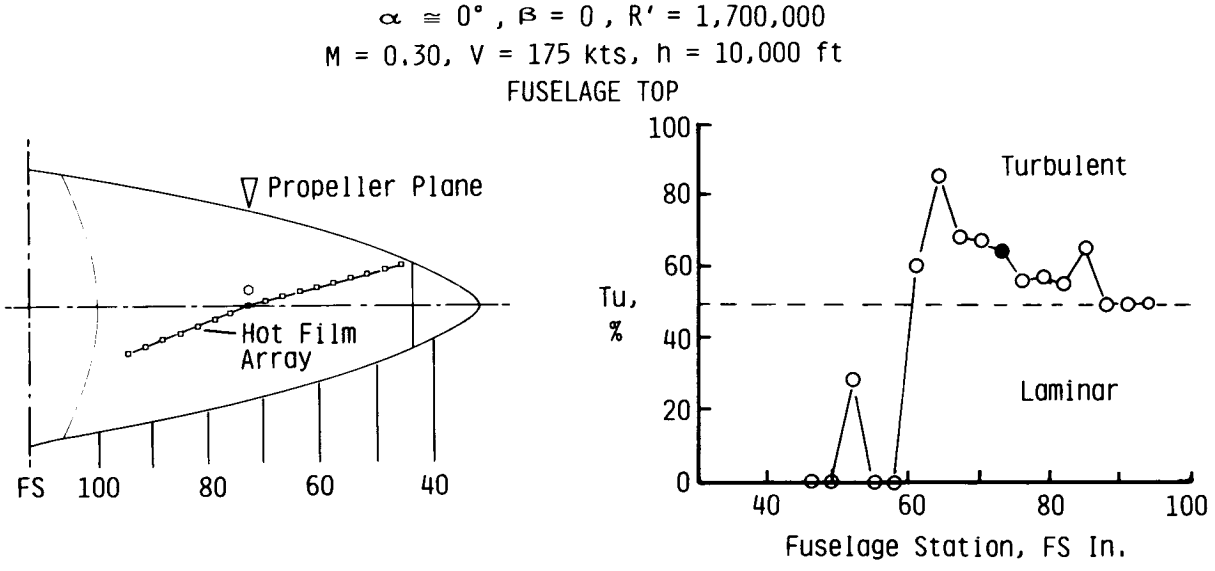

Figure 14a

T303 NLF FUSELAGE FLIGHT EXPERIMENT

Hot Film Boundary-Layer Turbulence Intermittency

$\alpha \cong 0°$, $\beta = 0$, $R' = 1{,}700{,}000$

M = 0.30, V = 175 kts, h = 10,000 ft

FUSELAGE STARBOARD SIDE

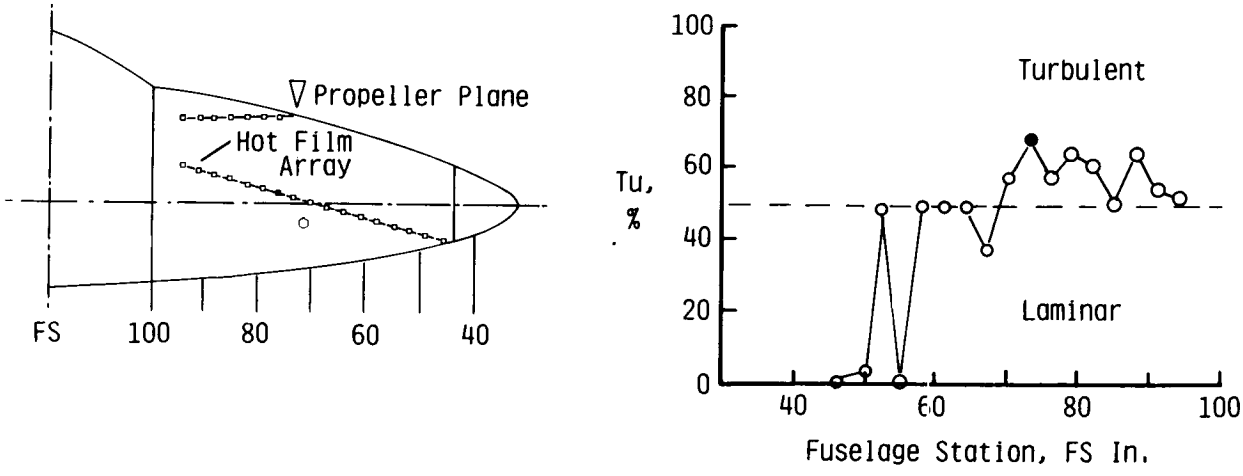

Figure 14b

T303 NLF FUSELAGE FLIGHT EXPERIMENT
HOT-FILM BOUNDARY-LAYER TURBULENCE INTERMITTENCY

Turbulent intermittencies obtained for both hot-film arrays are shown for a reduced unit Reynolds number R' = 800,000 at zero angle of attack in Figure 15a and 15b. Decrease in Reynolds number for this flight condition results in a large increase in laminar run on both top and side of the fuselage. Transition onset is indicated to occur behind the propeller plane, while intermittencies in the turbulent boundary layer beyond FS 90 grow to levels over 80 percent, in contrast to the levels indicated in Figures 14 at the higher unit Reynolds number.

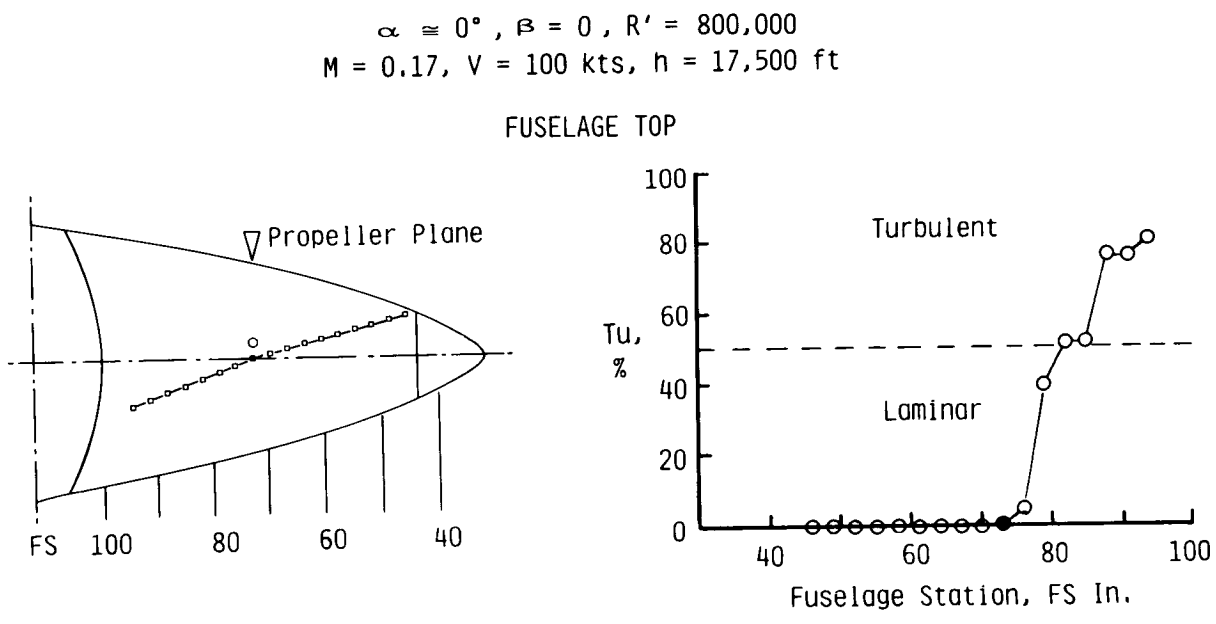

Figure 15a

T303 NLF FUSELAGE FLIGHT EXPERIMENT

Hot Film Boundary-Layer Turbulence Intermittency

$\alpha \cong 0°$, $\beta = 0$, $R' = 800{,}000$

$M = 0.17$, $V = 100$ kts, $h = 17{,}500$ ft

FUSELAGE STARBOARD SIDE

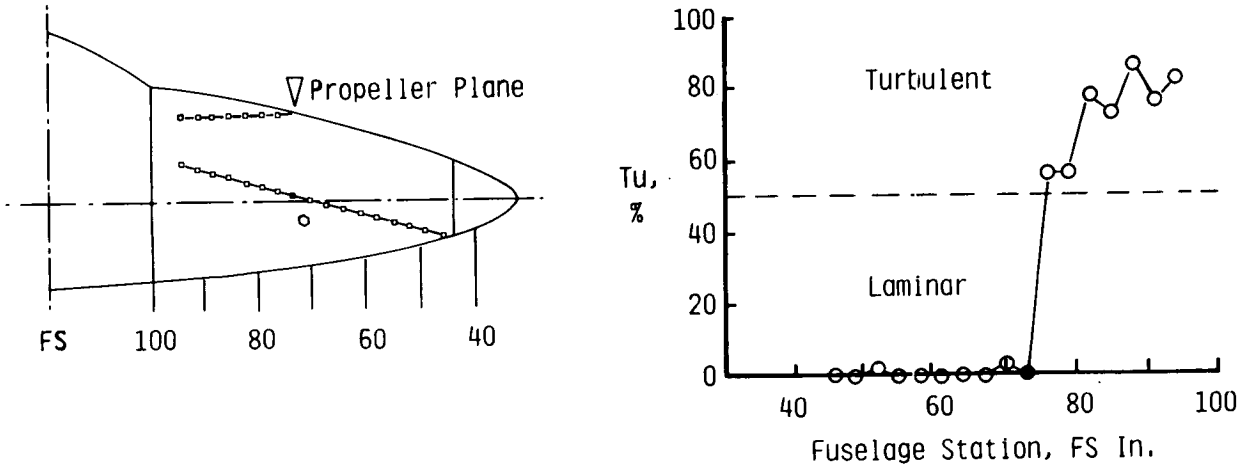

Figure 15b

T303 NLF FUSELAGE FLIGHT EXPERIMENT
PRELIMINARY FLIGHT-TEST RESULTS
CONTINUATION FLIGHT-TEST PROGRAM

The results from only a limited number of flights and initial data reduction are summarized in Figure 16a. Continuation of the flight program is planned to explore the location and mode of transition on this nonaxisymmetric fuselage shape under varying flight conditions as indicated in Figure 16b. The prototype airplane used in this program allows for extended glide flight with wind-milling propellers and stopped generators. Study of transition location without streamtube and noise effects of the propellers and generators provides an opportunity to assess acoustic receptivity phenomena in the boundary layer under study. Subsequent analysis of microphone and hot-film signals in time and frequency domain is planned to help understanding of the transition process under varying flight conditions. Analysis of stability of the laminar boundary layer over the fuselage nose using a full three-dimensional method can determine in detail the significance of cross flow in the location of transition as measured with the hot films.

Preliminary Flight Test Results

- Agreement pressure distribution calculation with measurement at α=0° (β=0°)
- Observed extent of laminar boundary layer at α=0° (β=0°) is 2.5 to 4.5 ft along surface: R_{TR} = 2.0-5.0 million
- Calculated T.S. amplification factor is 6-9 in observed transition range

Figure 16a

Continuation Flight Test Program

- Planned flight matrix
  $-2° < \alpha < 7.5°$
  $-10° < \beta < 10°$
  $750{,}000 < R' < 2{,}500{,}000$
  Propeller/generator power setting/RPM
  (including glide flights)
- Spectral analysis hot film and microphone signals
- Identification transition mode(s)

Figure 16b

EFFECT OF FLIGHT ALTITUDE ON UNIT REYNOLDS NUMBER

The transition observations over the nonaxisymmetric fuselage shape obtained in this flight program are obtained at low Mach numbers (0.20 to 0.35) and flight altitudes from 5,000 to 20,000ft, resulting in unit Reynolds numbers of 750,000 to 2,500,000 per foot (Figure 17). Typical flight conditions of subsonic (and supersonic) transports occur at comparable unit Reynolds numbers, however, at considerably higher flight altitudes and Mach numbers. As demonstrated in Reference 1 for a business-jet type body shape, Tollmien-Schlichting stability of the axisymmetric laminar boundary layer is greatly increased when Mach number increases to 0.80 as compared to incompressible conditions. Transition length Reynolds numbers of 20 million (see Figure 5) and higher seem possible at high-subsonic flow conditions when the favorable effect of flow compressiblity on boundary-layer stability is included. Study of effects of nonaxisymmetry and noise on transition location over a practical fuselage shape, which are investigated in the present flight program, is relevant to assess the achievability of substantial amounts of sufficiently stable laminar flow over the geometries indicated in Figure 1.

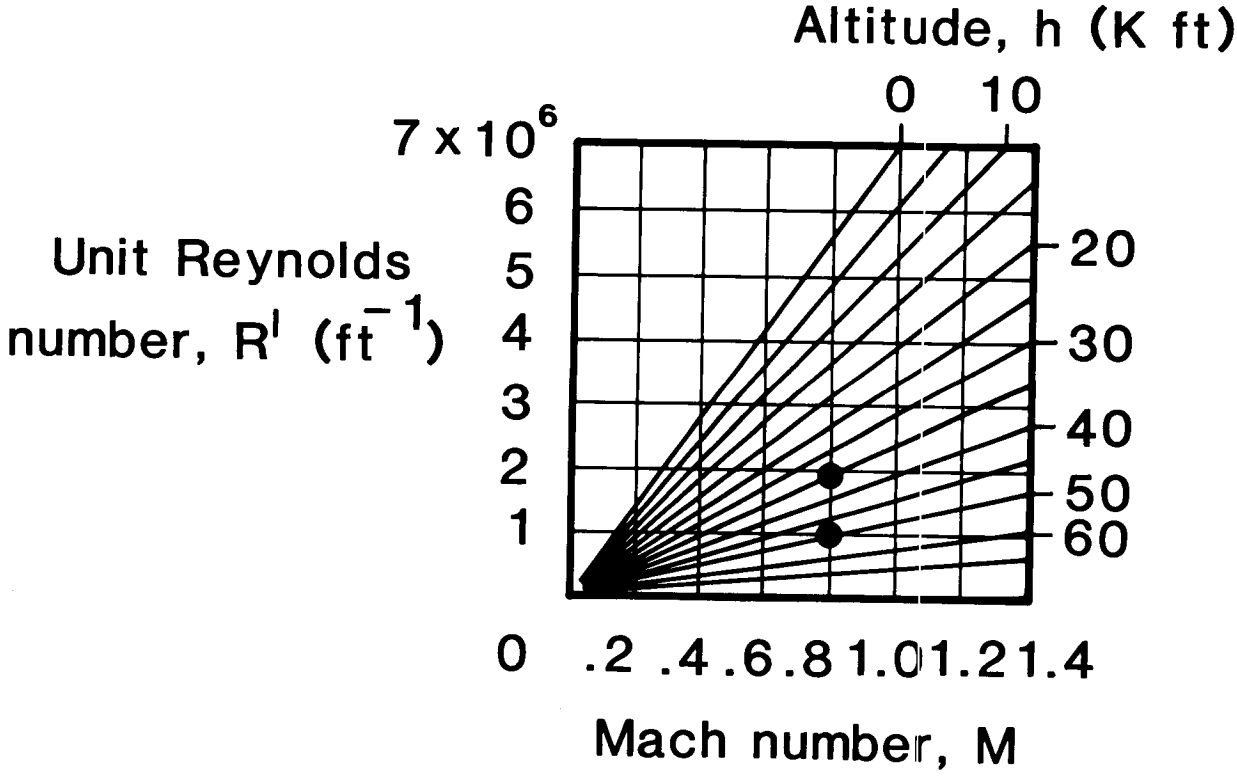

Figure 17

RESEARCH NEEDS FOR LAMINAR FLOW OVER FUSELAGES

The present study is the first flight investigation of stability of natural laminar flow over a practical nonaxisymmetric fuselage shape under varying free-stream conditions. Figure 18 indicates areas where further work is needed to understand the transition process over nonaxisymmetric fuselage geometries and to define application limits for laminar flow over body shapes in a fashion similar to the limits currently emerging for laminar flow over swept and unswept lifting surfaces. Detailed microscopic boundary-layer development and boundary-layer stability measurements are needed on bodies at sufficiently high length Reynolds numbers in a large low-turbulence ground facility as well as in flight to assess adequacy of boundary-layer and boundary-layer stability calculation methods. Similarly, wind-tunnel and flight experiments are required to investigate the stability of laminar flow over nonaxisymmetric bodies at subsonic and supersonic flight conditions. Only very limited studies of effects of manufacturing imperfections on the stability of laminar flow over fuselage geometries have been published. Waviness and step tolerances derived for wing-like geometries (Reference 10) need to be assessed for fuselage geometries which in general are characterized by axial pressure gradients that are less favorable than pressure gradients present over wings.

- Development and application of 3-D boundary-layer and boundary-layer stability codes for fuselage geometries
- Detailed 3-D boundary-layer measurements on bodies at high Reynolds numbers
- Body experiments at compressible flow conditions
- Study of NLF manufacturing tolerances for body geometries

Figure 18

REFERENCES

1. Vijgen, P. M. H. W., Dodbele, S. S., Holmes, B. J., and Van Dam, C. P., "Effects of Compressibility on Design of Subsonic Natural Laminar Flow Fuselages," AIAA 4th Applied Aerodynamics Conference, San Diego, June 1986. AIAA Paper 86- 1825CP.

2. Georgy-Falvy, D., "Effect of Pressurization on Airplane Fuselage Drag," J. of Aircraft, Vol. 2, No. 6, 1965, pp. 531-537.

3. Dodbele, S. S., Van Dam, C. P., Vijgen, P. M. H. W., and Holmes, B. J., "Shaping of Airplane Fuselages for Minimum Drag", AIAA 24th Aerospace Science Meeting, Reno, 1986. AIAA Paper 86-0316, also: J. of Aircraft, Vol. 24, No. 5, May 1987, pp. 298-304.

4. Williams, K.L., Vijgen, P. M. H. W., and Roskam, J. R., "Natural Laminar Flow and Regional Aircraft," SAE Paper 850864, 1985 SAE General Aviation Aircraft Meeting & Exposition, Wichita, Kansas. Published in SAE Transactions, Vol. 4, 1985.

5. Hastings, E., Schoenster, J., Obara, C., Jones, M., Dodbele, S., Faust, G., and Mungur, P., "The NLF Nacelle Flight Experiment", Symposium on Natural Laminar Flow and Laminar Flow Control Research, NASA CP 2487, 1987, pp. 887-921.

6. Boltz, F.W., Kenyon, G.C., and Allen, C.Q., "The Boundary-Layer Transition Characteristics of Two Bodies of revolution, a Flat Plate and an Unswept Wing in a Low-Turbulence Wind Tunnel," NASA Technical Note D-309, April 1960.

7. Carmichael, B. H., "Underwater Vehicle Drag Reduction Through Choice of Shape," AIAA Second Propulsion Joint Specialist Conference, June 1966, AIAA Paper 66-657.

8. Maskew, B., "Prediction of Subsonic Aerodynamic Characteristics - A Case for Low-Order Panel Methods," J. of Aircraft, Vol. 19, No.2, 1982, pp. 157-163.

9. Harris, J., and Iyer, V., "Numerical Solutions of the Compressible 3-D Boundary-Layer Equations for Aerospace Configurations with emphasis on LFC," Symposium on Natural Laminar Flow and Laminar Flow Control Research, NASA CP 2487, 1987, pp. 517-545.

10. Holmes, B.J., Obara, C.J., Martin, G.L., and Domack, "Manufacturing Tolerances for Natural Laminar Flow Airframe Surfaces," SAE Paper 850863, 1985 SAE General Aviation Aircraft Meeting & Exposition, Wichita, Kansas.

11. Cooke, J.C., and Hall, M.G., "Boundary Layers in Three Dimensions", in Progress in Aeronautical Sciences, Volume 2, Boundary Layer Problems, Ed. by A. Ferri, Pergamon, 1962.

12. Harris, J.E., and Blanchard, D.K., "Computer Program for Solving Laminar, Transitional, or Turbulent Compressible Boundary-Layer Equations for Two-Dimensional and Axisymmetric Flow," NASA TM-83207, Feb. 1982.

13. Srokowski, A.J., and Orszag, S.A., "Mass Flow Requirements for LFC Wing Design", AIAA Paper 77-1222, 1977.